Catal Lett (2009) 130:177–184
DOI 10.1007/s10562-009-9847-8

The Role of the Promoters in Cu Based Catalysts for Methanol Steam Reforming

Gui-Sheng Wu · Dong-Sen Mao · Guan-Zhong Lu · Yong Cao · Kang-Nian Fan

Received: 16 April 2008 / Accepted: 7 January 2009 / Published online: 17 January 2009

Abstract Effects of promoters such as zirconia and zinc oxide to copper catalysts have been studied in methanol steam reforming (MSR) reaction at 260 °C. The catalytic activity and stability of copper are improved by promoters, especially zirconia. The results of S_{BET} and S_{Cu} represent that both promoters can increase S_{BET} of catalysts from 0.26 to 0.28–0.99 m^2/g and S_{Cu} of them from 0.13 to 0.21–0.25 m^2/g and XRD further illustrate that they can stabilize the crystal size of copper in process of reduction and reaction. Besides, XPS results indicate that both ZnO and ZrO_2 can stabilize Cu^+ species and promote the catalytic activity for MSR. In addition, the rich surface hydroxyl species on ZrO_2/Cu account for its superior catalytic performance to ZnO/Cu and Cu.

Keywords Methanol steam reforming (MSR) · ZnO/Cu · ZrO_2/Cu · Cu^+ species · Surface hydroxyl

1 Introduction

The steam reforming of methanol for H_2 production over alumina-supported Cu/ZnO catalysts has attracted enormous interest in the development of fuel cell powered devices, especially for mobile applications [1, 2]. A large variety of catalytic materials for the steam reforming of methanol have been reported in the literature. Among them, copper-containing catalysts such as CuO/ZnO and CuO/ZnO/Al_2O_3, which are traditionally used for methanol synthesis and low-temperature water gas-shift reaction, have been the most frequently studied [3, 4]. Despite their high activity and selectivity for MSR, shortcomings of the conventional Cu/ZnO-based catalysts have been noted as the problems with long-term stability, low resistance to contaminants and the formation of poisonous CO as a byproduct [5]. Therefore, the development of new efficient catalyst systems that exhibit an improved long-term stability and selectivity for hydrogen production is highly desired.

In developing more suitable catalysts for MSR, CuZr-based catalysts have attracted considerable attention owing to their high activity and enhanced stability compared with conventional ZnO-supported counterparts [1, 6]. The eximious performances of zirconia containing catalysts have been attributed to a higher Cu surface area, better Cu dispersion, and improved reducibility of Cu [1, 6]. Besides, the interface between copper and zirconia has attracted more and more attention because particular electron interaction and synergistic effect occur [7–10]. Therefore various synthetic methods including coprecipitation of metal salts [7], impregnation of copper onto a zirconia support [8], the formation of amorphous aerogels and the polymer templating technique have been used [9, 10] with the aim of augmenting the interface between copper and zirconia by improving the copper dispersion or by restraining the crystallization of zirconia. Furthermore, it is also notable the catalytic activity of Cu/ZrO_2 for methanol synthesis or MSR increases with rise of the calcination or reduction temperatures in spite of the crystallization of zirconia and increase of copper crystal size [7, 10]. The accumulation of zirconia on the surface of catalyst is

G.-S. Wu (✉) · D.-S. Mao · G.-Z. Lu
Department of Chemical Engineering, Research Institute of Applied Catalysis, Shanghai Institute of Technology, 200235 Shanghai, People's Republic of China
e-mail: gswu@fudan.edu.cn

Y. Cao · K.-N. Fan
Department of Chemistry, Fudan University, 200433 Shanghai, People's Republic of China

observed due to migration of zirconia on the catalytic surface with rise of calcinations/reduction temperature [7, 10]. For CuZnAl catalysts, the similar correlation of catalytic activity and the reduction temperature is observed, which is also accounted for by the encapsulation of ZnO on the surface of Cu/ZnO [11]. In order to further clarify ZnO effects, Cu crystal surface modified by ZnO is also studied using surface science experiments [12, 13] and theoretical calculation [14].

Even though the extensive studies have been devoted to the mechanism of catalytic reactions mediated by copper based catalysts, many questions remain open. The Cu^0 or Cu^+ species is proposed to be active sites alone [1, 6]. In other studies, zirconia is proposed to participate in the reaction and form the active site with copper species [7, 10].

In the present work, the model catalysts, pure copper particles doped by zirconia or by zinc oxide, are designed, whose catalytic activities for MSR were investigated to elucidate the relation between the catalytic actives and catalytic surface structure, attempting to answer the following questions: (1) in ZnO and ZrO_2, which is more remarkable to promote the catalytic activity of copper? (2) How does the electric properties of copper vary doped with promoters? (3) What is the crucial factor to promote the catalytic performances.

2 Experimental Section

2.1 Catalytic Preparation

Pure copper catalysts were prepared by calcination of copper nitrate at 400 °C for 4 h. ZrO_2/Cu (ZrO_2: 10 wt%) and ZnO/Cu (ZnO: 10 wt%) were obtained by impregnation method. Briefly, CuO decomposed from $Cu(NO_3)_2$ was impregnated in the solution (5 M) of $Zr(NO_3)_4$ or $Zn(NO_3)_2$ for 10 h, followed by air drying at 120 °C for overnight and air calcinations at 400 °C for 4 h.

2.2 Catalytic Testing

The catalytic activity for MSR was measured in a continuous flow, fixed-bed *U*-shape quartz reactor under atmospheric pressure. 200 mg sample (40–60 mesh) was used, which was reduced in flowing H_2/Ar (30 mL/min) at 260 °C in advance. The reaction feed (60 mL/min) was obtained by converging two routes of He, which passed through the bubblers (at 50 °C) of water and methanol, respectively. The ratio of methanol and water is 1.2, which was achieved by adjusting the flux ratio of He through two bubblers filled with water and methanol, with 1.85 g/(hg) of GHSV (gas hour space velocity). The tailor gas was on-line analyzed with quadrupole mass spectrometer (QMS200, Balzers OmniStar). In the process of reaction, the feed rate was kept constant and the reaction time in Fig. 1 is defined as the time on stream.

2.3 Sample Characterizations

Powder X-ray diffraction (XRD) patterns were acquired on a Bruker AXS D8 Advance X-ray diffractometer using Cu-Kα radiation (0.15418 nm). The tube voltage and current was 40 kV and 40 mA, respectively. Sample used for XRD was on-line reduced at 260 °C for 1 h, and then was exposed in the flowing mixture of methanol and water at 260 °C for 1 h. The mean crystallite dimensions were obtained from the integral width of Cu (111) diffraction line using the Scherrer relation after correction for instrumental broadening with the Warren procedure [15]. The nitrogen isotherms and subsequently the multipoint Brunauer–Emmett–Teller (BET) surface areas (S_{BET}) were determined by N_2 adsorption at −196 °C in the Micromeritics TriStar 3000 apparatus, using a value of 0.164 nm^2 for the cross section of the nitrogen molecule. The surface of pure copper in the reduced catalyst was determined with the use of the reactive adsorption of N_2O at 90 °C according to the method described in [16]. The surface morphologies were observed by scanning electron microscopy (SEM, Philips XL 30). Before being transferred into the SEM chamber, the sample with ethanol was dispersed on the sample holder and then quickly moved into the vacuum evaporator (LDM-150D) in which a thin gold film was deposited after drying in vacuo. X-ray photoelectron spectra (XPS, Perkin Elmer PHI5000C) were recorded with Al-Kα radiation as the excitation source (hv = 1,486.6 eV). The sample pressed into a self-supported disc was mounted on the sample plate. Then it was

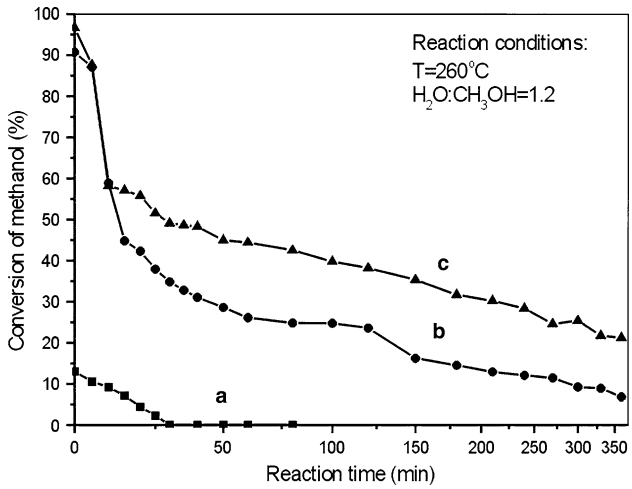

Fig. 1 The catalytic activity for the methanol steam reforming reaction: *a* Cu, *b* ZnO/Cu, *c* ZrO_2/Cu

degassed in the pretreatment chamber at 110 °C for 2 h in vacuo before being transferred into the analyzing chamber where the background pressure was lower than 2×10^{-9} Torr. All the binding energy (BE) values referenced to the C 1 s peak of contaminant carbon at 284.6 eV with an uncertainty of ±0.2 eV. Before XPS test, the catalysts after reaction were protected in N_2 atmosphere, which was treated by Ar ion sputtering in XPS process in order to removing the surface oxides induced by transitory exposition in air. About 50 mg sample was placed between two layers of the quartz sand of *U*-type quartz reactor for temperature programmed reduction (TPR) studies. TPR analyze was carried out in a flow of 5 vol% H_2/Ar (50 mL/min) from ambient temperature to 600 °C at a heating rate of 15 °C/min. The H_2 consumption was recorded by monitoring m/e signal of two with an on-line quadrupole mass spectrometer.

3 Results

3.1 Activity

The activity data for MSR (in Fig. 1) represent that the initial conversion of methanol of Cu is about 14%, which gradually decreases to 0% after 30 min. In contrast, the initial conversions of ZnO/Cu and ZrO_2/Cu catalysts are beyond 90%, which rapidly decrease to 37.9 and 51.6% after 25 min, respectively. Despite of further continuous decrease of conversion of methanol with reaction time, promoted Cu catalysts, especially ZrO_2/Cu, show much higher stability than Cu. These results illustrate that both promoters can promote the catalytic activity and stability, in which the promotion of zirconia is more remarkable.

3.2 The Basis Properties of Catalysts

The data in Table 1 indicate that the S_{BET} and S_{Cu} of copper catalyst are 0.26 and 0.13 m^2/g, respectively. Introduction of ZnO or ZrO_2 can increase S_{Cu} and S_{BET} of catalyst. Among others, effect of zirconia is more prominent, with S_{BET} and S_{Cu} being 0.99 and 0.25 m^2/g, respectively.

3.3 XRD Results

Copper of all catalysts is in the form of CuO before reduction (Fig. 2), and their crystallization is almost the same judging from the crystal sizes of CuO shown in Table 1. Besides, the evident diffraction peaks of ZnO appear in pattern of ZnO/Cu while those of ZrO_2 phase are not identified in pattern of ZrO_2/Cu, illustrating the zirconia is high dispersed state or amorphous in ZrO_2/Cu. Because XRD patterns of catalysts after reduction and after reaction are almost identical, only the results after reaction are displayed in Fig. 3. It indicates that CuO in all catalysts is reduced into metallic copper after reduction and after reaction. The data in Table 1 also illustrate that the copper crystal sizes of ZrO_2/Cu or ZnO/Cu after reduction and after reaction is slightly small than reduced Cu, indicating of the stabilization role of promoters to the copper crystal

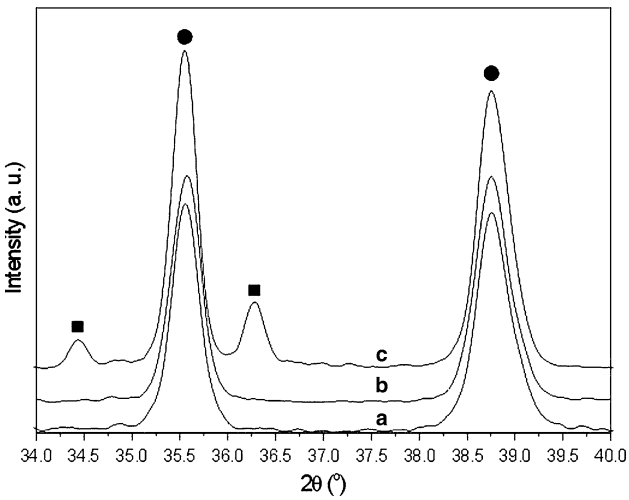

Fig. 2 XRD patterns [CuO (●), ZnO (■)] of the catalysts before the reactions: *a* Cu, *b* ZrO_2/Cu, *c* ZnO/Cu

Table 1 The basic properties of catalysts

Sample	S_{BET}(m^2/g)	S_{Cu}(m^2/g)[a]	Crystal size of Cu[b] (nm)			Reduction degree[d] (%)
			Before reaction	After reduction[c]	After reaction[c]	
CuO	0.26	0.13	22.5	29.9	31.5	100
ZnO/Cu	0.28	0.21	21.6	28.9	29.6	103
ZrO_2/Cu	0.99	0.25	22.9	27.5	26.0	116

[a] Determined with the use of the reactive adsorption of N_2O at 90 °C

[b] Determined by XRD

[c] The temperatures of reduction and reaction are 260 °C, respectively

[d] Calculated assuming that CuO was reduced to Cu^0

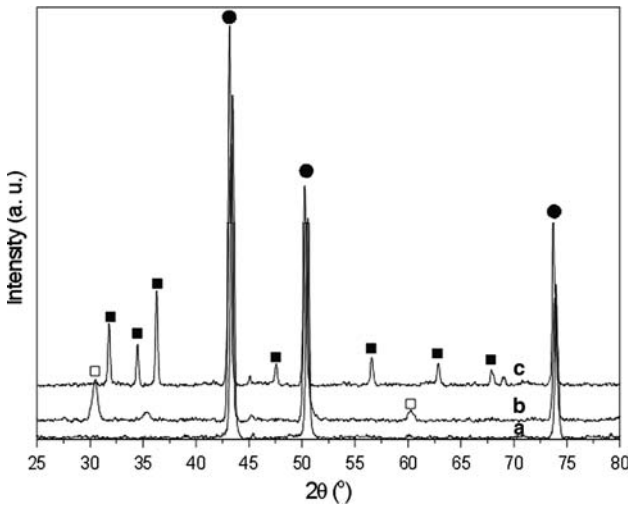

Fig. 3 XRD patterns [CuO (●), ZnO (■), t-ZrO_2(□)] of the catalysts before the reactions: *a* Cu, *b* ZrO_2/Cu, *c* ZnO/Cu

size in the process of reduction or reaction. In addition, it is also notable that the copper crystal size of ZrO_2/Cu after reaction is smaller than that after reduction, further illustrating the particular stabilization role of zirconia.

3.4 TPR Results

Although TPR profiles of three catalysts both display a single reduction peak (see Fig. 4), corresponding to reduction of CuO to Cu, two types of promoters have the different effect to the reduction of copper. ZrO_2 can promote the reduction of CuO remarkably, reflected by the phenomena that the maximum of ZrO_2/Cu reduction peak decreases by about 20 °C and that the reduction peak becomes narrow. Although the maximum of reduction peak of ZnO/Cu almost identical with that of Cu,

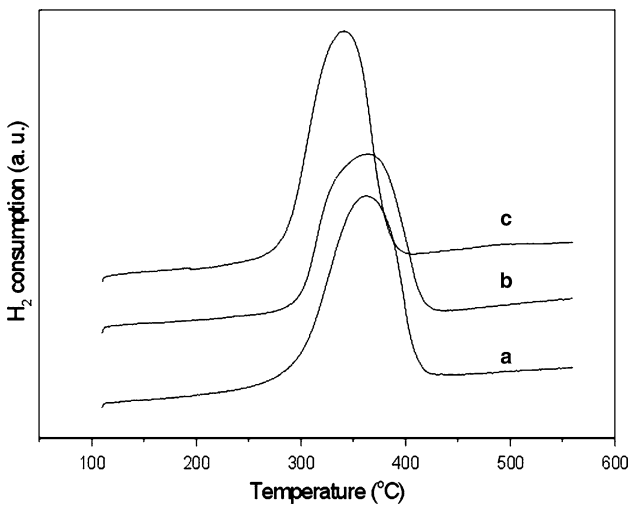

Fig. 4 TPR profiles catalyst: *a* Cu, *b* ZnO/Cu, *c* ZrO_2/Cu

broadening of reduction peak indicates that the reduction of copper becomes difficult. The amount of H_2 consumed during the reduction process is used to determine the reduction degree of copper in catalysts assuming that CuO is reduced to Cu^0. It is found that the reduction degree of ZrO_2/Cu and ZnO/Cu is 116 and 103% (in Table 1), respectively, indicating that the species of zirconia and zinc species also consume hydrogen in the process of reduction.

3.5 SEM Results

The morphological images from SEM are represented in Fig. 5. SEM image of Cu (Fig. 5a) is characteristic of short bars stacked randomly, which badly aggregate and form the honeycomb-like morphology (Fig. 5b) after reaction of MSR. Zirconia doped on CuO is highly dispersed (see Fig. 5c), with slight change of CuO configuration. After reaction of MSR, the aggregation of Cu in ZrO_2/Cu is greatly restrained by the zirconia, with amorphous zirconia of multi-pore structure wreathing on the surface of copper (Fig. 5d). In contrast, the larger ZnO particles on the surface of CuO are identified on the surface of ZnO/Cu before reduction (Fig. 5e). After reaction (Fig. 5f), the morphology of ZnO/Cu is flatter with fewer pores than that of Cu and ZrO_2/Cu. Furthermore, it is difficult to distinguish the copper from zinc species on the surface of ZnO/Cu after reaction, indicating that the homogeneous species of copper and zinc are formed.

3.6 XPS Results

To shed light onto the change of surface species of copper catalysts promoted with ZrO_2 or ZnO, XPS studies were carried out (see Fig. 6). From the inspection of the shape of the spectra and the values of the Cu 2p BEs and Auger parameters summarized in Table 2, it can be concluded there exists the single Cu^0 specie on the surface of Cu, which is characterized by the maximum of the main photoelectron peak at 932.5 eV, and the value of the Auger parameter at 1,850.6 eV [17]. For ZrO_2/Cu and ZnO/Cu, there also exists Cu^+ species besides the Cu^0 species, featured by shift to 1,848.2 eV of Auger parameter of the main peak [17]. It is worth noting that there appears the shoulder peak at BE of 934.5 eV for Cu $2p_{3/2}$ peak of ZrO_2/Cu, which is higher about 1 eV relative to the BE of main peak of Cu^{2+} and might be attributed to Cu species interacting strongly with zirconia. On the Cu/ZrO_2 with low copper loading, the XPS of Cu also displayed a single peak at about 934 eV [9] because of a strong interaction in terms of charge transfer from copper to nearby oxygen ligands of ZrO_2. Our results by theoretical calculation also illustrated the copper atoms coordinated by a $-OZrO_x(OH)_{3-x}$ hold 0.6–0.9 positive charge [18]. It can be envisioned that the

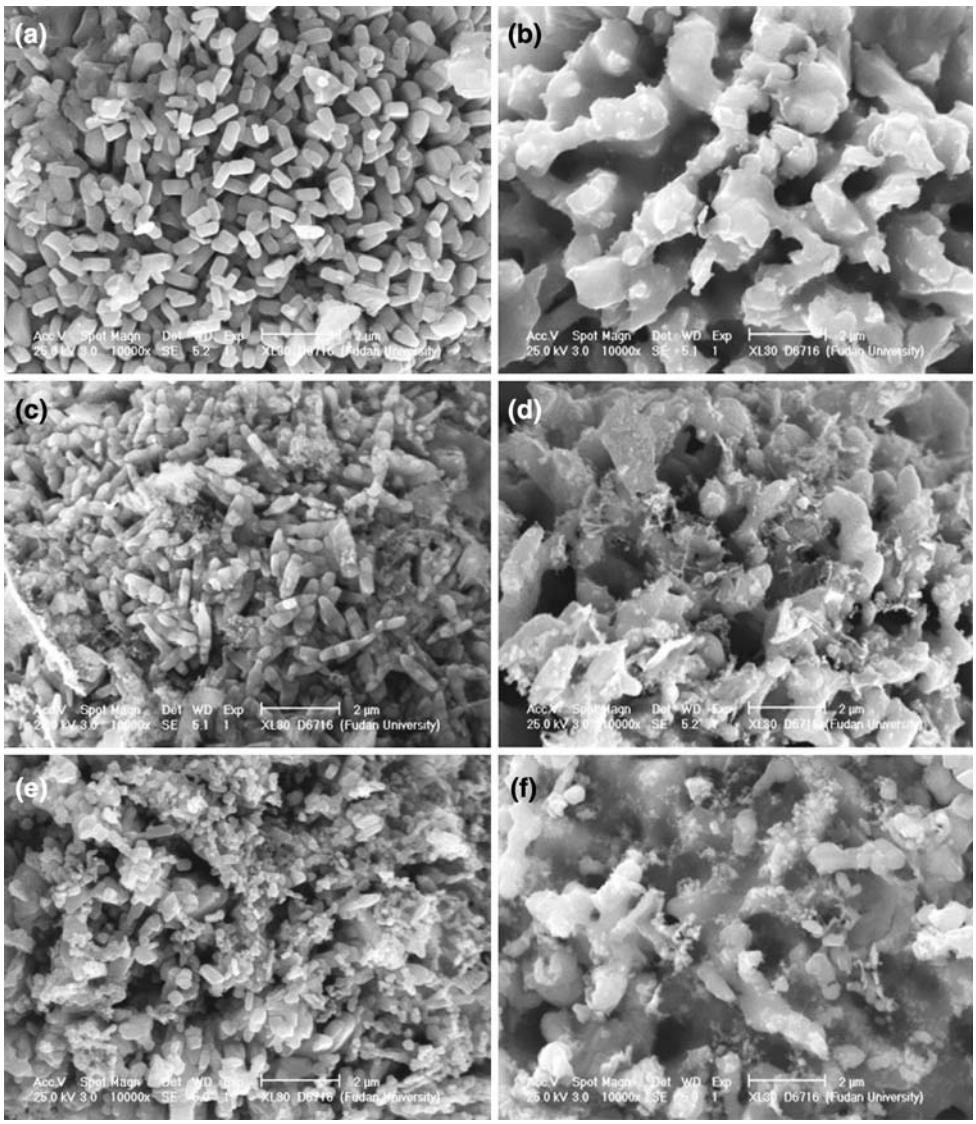

Fig. 5 SEM of catalysts: **a** Cu as prepared, **b** Cu after reaction, **c** ZrO_2/Cu as prepared, **d** ZrO_2/Cu after reaction, **e** ZnO/Cu as prepared, **f** ZnO/Cu after reaction

copper atom coordinated with more $-OZrO_x(OH)_{3-x}$ will transfer more charge to near oxygen atoms and that its BE will shift to higher value.

O 1 s XPS of ZnO/Cu and ZrO_2/Cu are also investigated, which are displayed in Fig. 7 and Table 3. All peaks are characterized by wide peaks indicating of the superposition of multi-peaks. According to the position of the different O species in literature, the O 1 s peaks are separated into three peaks at about 532.7, 531.5, 528.9 eV, which corresponds to O of $-OH$ (O_I), O of ZnO, ZrO_2 or Cu_2O (O_{II}) and O of CuO (O_{III}), respectively [17, 19]. After reaction, the XPS of O 1 s shift to higher position due to lose of O_{III} species. The relative O contents tabulated in Table 3 show that $O_I/(O_I + O_{II})$ of catalysts before and after reaction only shows slight change, indicating that the states of ZnO and ZrO_2 are relative stable in the process of reduction and reaction. Furthermore, the $O_I/(O_I + O_{II})$ of ZrO_2/Cu is about 3.8 times as high as that of ZnO/Cu, illustrating much richer hydroxyl presents on the surface of ZrO_2/Cu.

4 Discussion

As catalytic supporter, both zirconia and zinc oxide are often used in various catalysts systems. However, ZrO_2/Cu has exhibited the higher activity and selectivity than ZnO/Cu in various reactions such as Fischer–Tropsch synthesis [20, 21], methanol synthesis [22, 23], and hydrodesulfurization [24], which have attributed to the zirconia properties of high surface area, high thermal stability and the amphoteric character [20–24]. The data of S_{BET} and XRD in the case also show that both promoters can improve the surface area of catalysts, stabilize the crystal size of copper and prevent copper particles from aggregation in the process of reaction. SEM results further show that zirconia is

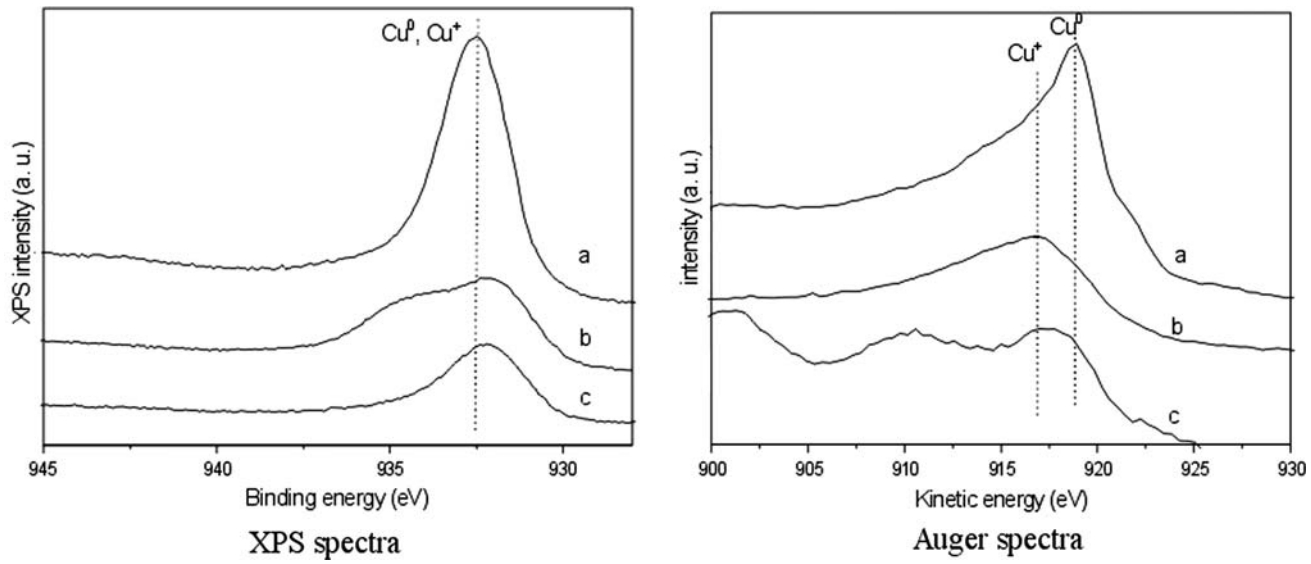

Fig. 6 Cu XPS and Cu Auger spectra pf catalydtd, *a* Cu, *b* ZrO_2/Cu, *c* ZnO/Cu

Table 2 Binding energies (eV), fwhm and Auger parameters of Cu $2p_{3/2}$ for copper catalysts

Sample	Oxide			After reaction	
	Satellite peak (eV)[a,b]	Main peak (eV)[a,b]	I_m/I_s^c	Main peak[a]	α'^d
Cu	942.1(4.6)[d]	933.7(3.7)[d]	2.18	932.5	1,850.6
ZrO_2/Cu	941.2(5.1)	932.9(4.6)	1.82	932.2	1,848.2
ZnO/Cu	941.5(3.8)	933.0(3.8)	2.40	932.3	1,848.2

[a] The position of binding energy

[b] The numbers in parentheses are full width at half-maximum (FWHM)

[c] The intensity ratio of main peak and satellite peak

[d] The Auger parameter which is the sum of BE of Cu 2p and KE of Auger peak

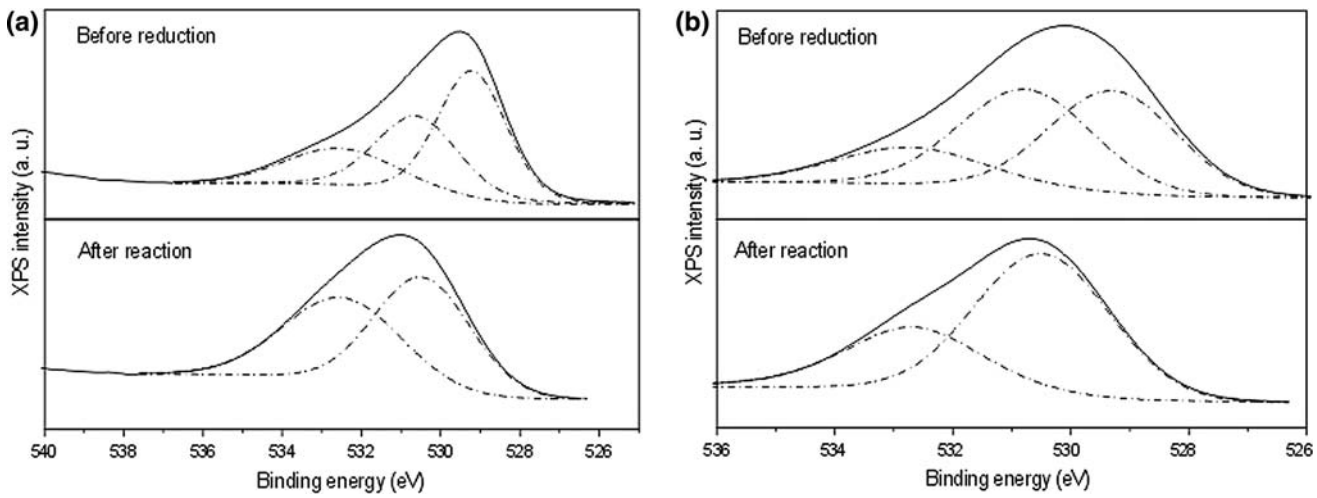

Fig. 7 O 1 s XPS of catalysts, **a** ZrO_2/Cu, **b** ZnO/Cu

Table 3 The binding energies (eV) of O 1 s for catalysts

Sample	State	BE of O 1 s (ev)			$O_I/(O_I + O_{II})$ (%)	$O_I/(O_I + O_{II} + O_{III})$ (%)
		O_I	O_{II}	O_{III}		
ZrO_2/Cu	Oxide	532.7	531.5	528.9	18.4	11.8
	After reaction	532.7	531.5		16.9	–
ZnO/Cu	Oxide	532.6	530.8	289.8	61.9	34.3
	After reaction	532.7	530.5		64.6	–

amorphous on ZrO_2/Cu, its promotion to the catalytic structure is more remarkable than that of ZnO. It is still notable that S_{BET} of ZrO_2/Cu is only 0.73 m^2/g larger than that of Cu, which might be due that zirconia is doped by impregnation and its loading is little. These results illustrate that it does not seem adequate to account for the remarkable improvement of catalytic activity and stability only through increase of S_{BET} and S_{Cu} as well as decrease of crystal size of copper. Accordingly, other factors to promote the catalytic activity should be taken account into.

Although a linear correlation between copper surface area and methanol synthesis activity has been observed by Chinchen et al. [25], more and more evidences have proved that Cu^+ [26] and Cu^0–Cu^+ [27] should be the active sites for methanol synthesis. Introduction of little amount of CO_2 or O_2 in feed can maintain the concentration of Cu^+, which can promote the catalytic activity remarkably [28, 29]. More recently, it is also found Cu/ZrO_2 catalyst reduced in hydrogen shows the initially low activity for MSR, whose activity is remarkably promoted with temporary exposition in oxygen of catalyst [30]. Oguchi et al. [31, 32] also proposed that the catalytic activity of Cu/ZrO_2 for MSR is approximate linear relation with its surface oxygen content. Besides, it also found that copper species on Cu/ZrO_2 with high activity are mostly the state of Cu^+ using XRD and EXAFS methods [31, 32]. Furthermore, the surface science experiments also prove that methanol or CO on clean single-crystal Cu surfaces tends to show little or no reactivity and the surface oxygen must exist on the surface of Cu crystal surface in order to facilitate the adsorption of methanol [33]. In our case, the results of XPS and Auger spectra also represent that Cu^+ dominates on the surface of ZrO_2/Cu and ZnO/Cu, which might be another reason for enhanced catalytic activity and stability. The results of our previous work [34] and other works [35, 36] show that there exist rich oxygen vacancies on the surface of zirconia and ZnO, which can stick the oxygen atom of Cu_2O and stabilize Cu^+ species. Reduction degrees of ZnO/Cu and ZrO_2/Cu determined by TPR in Table 1 are beyond 100%, further evidencing that rich oxygen vacancies are formed in the process of reduction. In addition, the copper species strongly interacted with zirconia are also indicative of positive charge nature owing to charge transfer from copper to the vicinal O of ZrO_2.

Besides, Oguchi et al. [31, 32] also suspect the hydroxyl on the surface of zirconia can improve the stability of CuO/ZrO_2 for MSR reaction. TPD results of water show that zirconia can effectively dissociate water even at 260 °C to form hydroxyl, which can react with adsorbed methanol to form CO_2 and H_2 and hinder oxygen species consumption on the surface of copper [37]. On the contrary, pure copper particles hardly display any desorption of water [37]. In Pt catalyst, similar opinion is also proposed that the Pt–OH species obtained from water dissociation react with adsorbed methoxide to produce CO_2 and H_2 [38]. On the basis of O contents of different types from XPS in Table 3, it is also shown that the hydroxyl of ZrO_2/Cu is about 3.8 times as high as that of ZnO/Cu, which might account for much higher catalytic activity and stability of ZrO_2/Cu than that of ZnO/Cu.

According to the discussion above, Cu^+ and surface oxygen as well as the physical structure of the catalysts are pertinent to the catalytic performance. Besides promotion of catalytic structure, zirconia species in ZrO_2/Cu are able to efficiently dissociate water to form surface hydroxyl, which not only react with adsorbed methanol or methoxide to produce CO_2 and H_2, but also maintain surface oxygen species on Cu to certain concentration. According, ZrO_2/Cu shows superior catalytic performance to ZnO/Cu and Cu.

In addition, it is also notable that while ZnO/Cu and ZrO_2/Cu are initially more active than Cu alone, the deactivation of all three catalysts is very pronounced. These phenomena might be ascribed to the preparation methods of the catalysts. The model Cu-based catalysts in the case are prepared by calcining and decomposing $Cu(NO_3)_2$, and the promoters with low loading (10%) are doped by impregnation. It is appear that copper particles are facile to congregate without the supporter, as is evidenced by the results of SEM. Even if promoter, ZnO or ZrO_2, can stabilize the crystal size of copper and prevent copper from aggregation, it can not still maintain the catalytic structure and activity well because impregnating the promoters can not disperse copper particles well. The aggregation of

copper might cause shrinkage of interface between copper and promoter and catalytic deactivation. Because of relative stable structure of ZrO_2 and role of surface hydroxyl, the deactivation rate of ZrO_2/Cu is less than that of ZnO/Cu and Cu.

5 Conclusion

The catalytic activity and stability of Cu catalyst is enhanced by both of ZrO_2 and ZnO promoters, which can not only enlarge the surface area of catalysts, stabilize the crystal size of Cu, and prevent Cu particles from aggregation in the process of reduction and reaction, but also stabilize the Cu^+ species on the surface of catalysts. Compared with ZnO, ZrO_2 is highly dispersed state on the surface of catalyst and holds rich surface hydroxyl, which can stabilize Cu^+ species and promote the catalytic activity. Therefore, ZrO_2/Cu manifests more excellent performance than Cu and ZnO/Cu for MSR.

Acknowledgments The financial supports from National Science Foundation of China (Grant No. 20503005, 20473021, 20421303, 20203003) and Shanghai Leading Academic Discipline Project (P1501) are gratefully acknowledged.

References

1. Matter PH, Braden DJ, Ozkan US (2004) J Catal 223:340
2. Reitz TL, Lee PL, Czaplewski KF, Lang JC, Popp KE, Kung HH (2001) J Catal 199:193
3. Hansen PL, Wagner JB, Helveg S, Rostrup-Nielsen JR, Clausen BS, Topsøe H (2002) Science 295:2053
4. Clausen BS, Schiøtz J, Gråbæk L, Ovesen CV, Jacobsen KW, Nørskov JK, Topsøe H (1994) Top Catal 1:367
5. Cheng W (1999) Acc Chem Res 32:685
6. Ramaswamy V, Bhagwat M, Srinivas D, Ramaswamy AV (2004) Catal Today 97:63
7. Wu G, Sun Y, Li Y, Jiao H (2003) J Mol Struct (Theochem) 626:287
8. Liu X-M, Lu GQ, Yan ZF (2005) Appl Catal A 279:241
9. Dongare MK, Dongare AM, Tare VB, Kemnitz E (2002) Solid State Ion 152–153:455
10. Sun Y, Sermon PA (1993) J Chem Soc Chem Commun 1242
11. Batyrev ED, van den Heuvel JC, Beckers J, Jansen WPA, Castricum HL (2005) J Catal 229:136
12. Nakamura J, Nakamura I, Uchijima T, Kanai Y, Watanabe T, Saito M, Fujitani T (1996) J Catal 160:65
13. Fujitani T, Nakamura I, Ueno S, Uchijima T, Nakamura J (1997) Appl Surf Sci 121:583
14. Hu Z-M, Nakatsuji H (1999) Chem Phys Lett 313:14
15. Warren BE (1941) J Appl Phys 12:375
16. Skrzypek J, Słoczynski J, Ledakowicz S (1994) Metanol Synthesis. Polish Scientific Publishers (PWN), Warszawa, p 45
17. Ghijson J, Tjeng LH, van Elp J, Eskes H, Westerink J, Sawatzky GA (1988) Phy Rev 38:11322
18. Wu G, Cao Y, Fan K (2009) J Phys Chem (submitted)
19. Okamoto Y, Fukino K, Imanaka T, Teranishi S (1983) J Phys Chem 87:3747
20. Bruce L, Mathews JF (1982) Appl Catal 4:353
21. Bruce L, Hope GJ, Mathews JF (1983) Appl Catal 8:349
22. Amenomiya Y (1987) Appl Catal 30:57
23. Fisher I, Bell AT (1998) J Catal 178:153
24. Hamon D, Vrinat M, Breysse M, Durand B, Jebrouni M, Roubin M, Magnoux P, des Courieres T (1991) Catal Today 10:613
25. Chinchen GC, Waugh KC, Whan DA (1986) Appl Catal 25:101
26. Klier K (1982) Adv Catal 31:243
27. Okamoto Y, Fukino K, Imanaka T, Yeyaniski S (1983) J Phy Chem 87:3747
28. Chen GC, Denny PT, Parker DG (1987) Appl Catal 30:33
29. Chen GC, Denny PT, Parker DG (1984) Prep Am Chem Soc Div Fuel Chem 29:178
30. Szizybalski A, Girgsdies F, Rabis A, Wang Y, Niederberger M, Ressler T (2005) J Catal 233:297
31. Oguchi H, Kanai H, Utani K, Matsumura Y, Imamura S (2005) Appl Catal A 293:64
32. Oguchi H, Nishiguchi T, Matsumoto T, Kanaia H, Utani K, Matsumura Y, Imamura S (2005) Appl Catal A 281:69
33. Varazo K, Parsons FW, Ma S, Chen DA (2004) J Phys Chem B 108:18274
34. Wu G, Wang L, Cao Y, Fan K (2006) Appl Sur Sci 253:974
35. Castricum HL, Bakker H, Linden B, Poels EK (2001) J Phys Chem B 105:7928
36. Fisher IA, Bell AT (1999) J Catal 184:357
37. Wu G, Wang L, Cao Y, Fan K (2009) Appl Catal (In press)
38. Laborde H, Lamy TM, Lamy C (1994) J Appl Electrochem 24:219